Electronic stopping power of ^{10}B in Si in random and ⟨100⟩ channeling directions

J. H. R. dos Santos, M. Behar, P. L. Grande, and H. Boudinov
Instituto de Física da Universidade Federal do Rio Grande do Sul, Avenida Bento Goncalves 9500, 91501-970, Porto Alegre, Brazil

R. Stoll, Chr. Klatt, and S. Kalbitzer
Max-Planck-Institut für Kernphysik, P. O. Box 103980, D-69029 Heidelberg, Germany
(Received 8 November 1996)

We report measurements of ^{10}B stopping powers in random and Si ⟨100⟩ directions. The measurements were carried out in the 500–9000 keV energy range for the channeling case and in the 300–800 keV for the random one. For the channeling measurements, the low energy data (500–800 keV) follow a v^s regime with $s=0.90\pm 0.06$ whereas, for the random data, $dE/dx\propto v^s$ with $s=1.1\pm 0.2$. Both results are in good agreement with the prediction of current theories. On the other side, the experimental random ^{10}B stopping power values (for energies up to 650 keV) are in fair agreement with the ones obtained from a scaling procedure by Ziegler, Biersack, and Littmark. However, for energies higher than 650 keV, slight but systematic differences are observed. [S0163-1829(97)03920-9]

I. INTRODUCTION

The slowing down of energetic ions penetrating the matter has been intensively studied for many years. As a consequence a large number of range measurements on a variety of projectile-target combinations have been performed in order to test current theories.[1] On the other hand in the same period of time much less stopping-power measurements have been performed and most of them have been done in random directions.[1] Furthermore, most of the published works on energy loss of energetic ions in channeling directions deal with protons and in less extent with He ions along the main Si axes.

An accurate knowledge of stopping powers for both random and channeling directions is important from both points of view: the underlying physics and practical applications. In the first case the data can test interatomic potentials and/or electronic excitation models used in range and atomic displacement calculations. From the practical point of view the data can be used as input of analytical or Monte Carlo type of programs that calculate depth distributions and damage produced by ions implanted into channeling and random directions of the matrix.

Usually, the energy loss of channeled ions has been performed by measuring the final energy of ions transmitted through thin single crystals. However the use of this method strongly depends on the preparation of homogeneous self-supporting single crystals. In particular, in order to measure the energy loss of ions heavier than protons or He at low or intermediate energies, extremely thin films must be employed.

In the past few years we have used an alternative method in order to determine the stopping of He ions channeled along the Si ⟨100⟩ and ⟨110⟩ directions.[2–4] In this way, the channeling energy loss before the backscattering can be obtained almost directly. The channeled ions are detected after being backscattered at some marker specially introduced for this purpose. Results for the energy loss along the ⟨110⟩ direction[2] have shown that this backscattering technique yields channeling stopping powers well consistent with the ones obtained from transmission techniques.

The stopping power data for B in Si are scarce and incomplete. Concerning the channeling data the pioneering work of Eisen[5] for ^{11}B in Si which was performed in a very narrow energy range using the transmission technique should be mentioned. Later works[6–8] have used range measurements of B implanted in channeling directions to obtain the corresponding channeling stopping powers. Finally, it should be mentioned that the only available random stopping power data for ^{10}B in Si is the one given by the RSTOP subroutine of the TRIM program.[1] These data are not experimental, but were obtained by a scaling procedure as described in Ref. 1.

Most of the stopping-power tabulations[9,10] and semiempirical models[1] extrapolate their results from intermediate and higher energies to lower ones, using velocity dependencies which are based on simple models. This is due to the fact that there are no *ab initio* theories that can describe precisely the low energy electronic stopping processes for ions in metals, semiconductors, or insulators. In particular, the Firsov model[11] and the Lindhard electron-gas theory[12] predict a linear dependence of the electronic stopping power with the projectile velocity. More recently this behavior was corroborated by calculations performed for metals.[13–16]

Following our theoretical-experimental study[2–4] of He stopping in channeling directions we have investigated the stopping of ^{10}B in random and Si ⟨100⟩ directions. The channeling experimental study was performed using the backscattering method in a 500–9000 keV energy range. The contribution to the electronic stopping power due to valence electrons from the Si was calculated using the free electron model.[17] On the other side the random stopping-power measurements were performed in a much restricted 300–800 keV energy range. The present results are compared to the previously published ones[5–7] and discussed in terms of current calculations.

II. EXPERIMENTAL PROCEDURE

A. Channeling experiments

1. Experimental setup

We have used SIMOX (separation by implanted oxygen[18]) type samples consisting of thin Si ⟨100⟩ crystal layers on top of 5000 Å SiO_2 buried layers, produced in ⟨100⟩ Si wafers. Two different thin single crystal layers, 750 and 1500 Å thick, were used for the stopping-power measurements in the ⟨100⟩ channeling direction.

The samples were prepared at IBM, T.J. Watson Research Center, New York. They were thinned by thermal oxidation and chemical etching. For each experiment the sample was cleaned and etched to remove the native oxide film on the surface using a 10% HF acid just before the Rutherford backscattering spectrometry (RBS) measurements. Then, they were mounted on a three axis goniometer of 0.005° precision. The experiments were done in the 500–9000 keV energy range. For energies lower than 800 keV, the $^{10}B^{2+}$ beam was produced by the 400 kV ion implanter of the Institute of Physics at Porto Alegre. For energies higher than 800 keV, the boron beam was provided by the 3 MV tandem accelerator at the Max Planck Institute für Kernphysik (MPI-K), Heidelberg. In both cases the ^{10}B beam angular divergence was better than 0.03°.

The energy-loss measurements were carried out using the beam impinging on the sample at channeling and random directions. Based on a recent study[19] and taking as references the ⟨100⟩ axis ($\Psi = 0$) and the {100} plane ($\phi = 0$), we have chosen as a random direction the one defined by $\Psi = 6°$ and $\phi = 15°$. The backscattered ^{10}B particles were detected by Si surface barrier detectors. At Porto Alegre the measurements were carried out using three different backscattering geometries with the Si detector at 165, 130, and 120° with respect to the incident ^{10}B beam. At Heidelberg three different detectors were used, placed at different geometries, but always forming an angle of 165° with respect to the impinging beam direction. The overall resolution of the detection systems at Porto Alegre and Heidelberg was always better than 25 keV. In addition to the experiments done at different geometries, several sets of measurements were performed under the same conditions. In all the cases, the results were reproducible at a 5% level.

The energy difference between the Si/SiO_2 interface positions in the random and channeling RBS spectra gives the corresponding difference in the energy lost in the path before the backscattering. As will be described in the next section, this difference provides the information about the stopping power in the channeling direction. In addition to energy loss, the RBS technique also simultaneously yields information about the dechanneling of the ions traversing the sample.

2. Data analysis

Typical RBS random and channeling spectra in the Si ⟨100⟩ direction for 800 keV and 8 MeV are shown in Figs. 1(a) and 1(b). E_c and E_r are the detected energies of the ^{10}B backscattered particles at the Si/SiO_2 interface in the aligned and random incidence, respectively.

The detected energies (using the mean energy approximation[20]) are

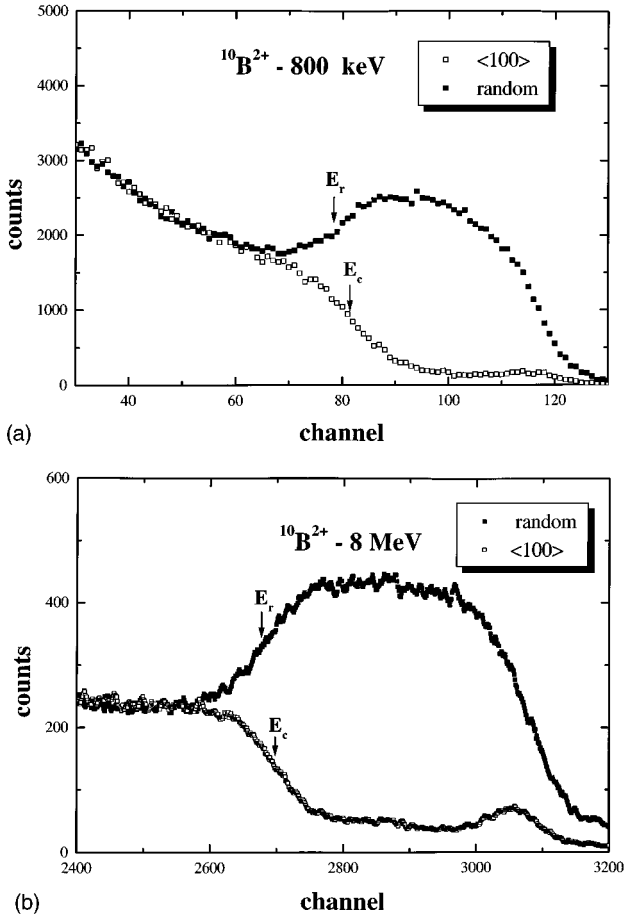

FIG. 1. (a) RBS random and channeling spectra in Si ⟨100⟩ direction for 800 keV ^{10}B ions. E_c and E_r are the detected energies of the backscattered particles at the Si/SiO_2 interface in the channeling and random directions, respectively. (b) Similar to (a) but for ^{10}B ions at 8 MeV of energy.

$$E_c = K\left[E_0 - \left.\frac{dE}{dx}\right|^{c}_{\overline{E}_{\rm in}} l_{\rm in}\right] - \left.\frac{dE}{dx}\right|^{r}_{\overline{E}_{\rm out}} l_{\rm out} \tag{1}$$

and

$$E_r = K\left[E_0 - \left.\frac{dE}{dx}\right|^{r}_{\overline{E}'_{\rm in}} l'_{\rm in}\right] - \left.\frac{dE}{dx}\right|^{r}_{\overline{E}'_{\rm out}} l'_{\rm out}, \tag{2}$$

where the prime $'$ refers to the random incidence, K is the kinematic Si factor, E_0 the incident beam energy, $(dE/dx)|^c$ the channeling specific energy loss (to be determined), and $(dE/dx)|^r$ the random one. $E_{\rm in}$ and $l_{\rm in}$($E_{\rm out}$ and $l_{\rm out}$) are the mean energy and length of the inward (outward) path. Combining Eqs. (1) and (2), we obtain

$$\left.\frac{dE}{dx}\right|^{c}_{\overline{E}_{\rm in}} = \left[\frac{KE_0 - E_c}{KE_0 - E_r}\left(\beta_1 + \frac{\cos\theta_1}{\cos\theta'_1}\right) - \beta_2\right]\left.\frac{dE}{dx}\right|^{r}_{\overline{E}'_{\rm in}}, \tag{3}$$

with

$$\beta_1 \equiv \frac{\left.\frac{dE}{dx}\right|^{r}_{\overline{E'_{\rm out}}}}{K\left.\frac{dE}{dx}\right|^{r}_{\overline{E'_{\rm in}}}} \frac{\cos\theta_1}{\cos\theta'_2}, \tag{4}$$

$$\beta_2 \equiv \frac{\left.\frac{dE}{dx}\right|^{r}_{\overline{E_{\rm out}}}}{K\left.\frac{dE}{dx}\right|^{r}_{\overline{E'_{\rm in}}}} \frac{\cos\theta_1}{\cos\theta_2}, \tag{5}$$

where θ_1 and θ_2 are the angles between beam and sample's normal and between sample's normal and detector directions, respectively.

An inspection of Eqs. (3), (4), and (5) shows that, for the present backscattering method, the determination of the Si crystal-layer thickness is not necessary. The energy loss of the channeled particles is obtained from geometrical factors, the detected E_c and E_r energies, and the specific energy loss in the random direction.

The E_c and E_r energies corresponding to the Si/SiO_2 interface were determined by fitting the channeling and random spectra with an algorithm which in addition to the error function (accounting for particle straggling and detector resolution) includes the Rutherford cross section dependence with the ion energy.

B. Random stopping power

1. Experimental setup

For this experiment, we have used a Bi marker implanted into an amorphized Si layer. First, we have determined the projected range R_p of the Bi ion distribution by using a He^{2+} beam. Then, we have determined the energy position of the same Bi marker by using a ^{10}B beam at different energies. With this information we were able to determine the random stopping powers of ^{10}B in Si as described below.

The sequence of experiments was the following: first we have amorphized a Si $\langle 100\rangle$ wafer using an Ar ($\phi = 2\times10^{14}$ at/cm^2, $E = 300$ keV) beam. After that, the sample was implanted with a 30 keV Bi beam at a fluence $\phi = 10^{15}$ at/cm^2, which is too low to modify the material, and, on the other hand, high enough to provide sensitivity for the backscattering experiments. Then, we have determined the range of the implanted Bi peak by using a 800 keV He^{2+} beam from the 400 kV ion implanter of Porto Alegre. The backscattered He^{2+} particles were detected by a Si surface barrier detector placed at 165° with respect to the beam direction. The overall electronic resolution was better than 12 keV. The range measurements were done at two different type of geometries: (a) with the sample at normal angle with respect to the beam (normal geometry) and (b) with the sample at five different angles ranging between 15 and 60° with respect to the beam (tilted geometry). A typical RBS spectrum for the normal geometry is shown in Fig. 2(a).

The energy to depth conversion was carried out using the recent He stopping power values reported by Niemann *et al.*[21] We have then obtained $R_p = 144\pm8$ Å. It should be stressed that the above value was obtained as an average of ten different range measurements taken at normal and tilted geometries. The quoted errors are the ones which arise from the statistical treatment of the individual measurements plus those which came from the uncertainties in the determination of the He stopping power (estimated at a 1% level).[21] Other sources of errors, such as geometry and ion beam energy uncertainties, are considered to be much less important.

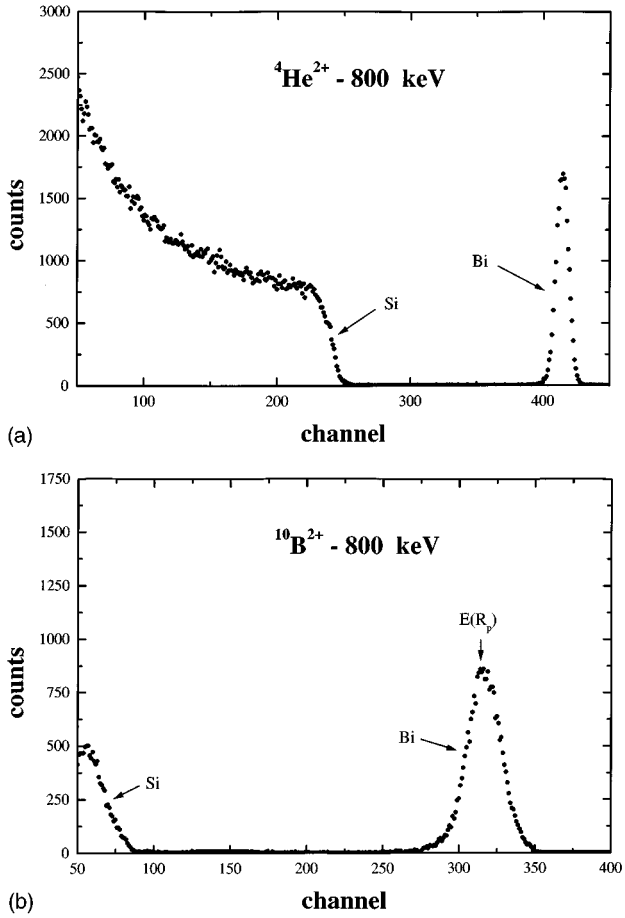

FIG. 2. (a) RBS spectrum of a 30 keV Bi marker implanted in Si obtained with a 800 keV, He^{2+} beam. (b) The same as (a) but obtained with a 800 keV ^{10}B beam.

In a next step, we have determined the energy position $[E(R_p)]$ of the Bi implanted peak by using ^{10}B beams with energies which varied between 350 and 800 keV. Figure 2(b) displays a RBS spectrum taken with a 800 keV ^{10}B beam. The energy position corresponding to the maximum of the Bi distribution is marked in this figure as $E(R_p)$. Considering the expression for the random energy-loss factor

$$[S(B)]^{\rm Si}_{\rm Bi} = \frac{K_{\rm Bi}E_0 - E(R_p)}{R_p}, \tag{6}$$

we can obtain the values for the electronic stopping power of ^{10}B in Si through the relation between the energy-loss factor and the energy loss per unit length dE/dx (in the surface energy approximation[20]):

$$[S(B)]^{\rm Si}_{\rm Bi} = \frac{K_{\rm Bi}}{\cos\theta_1}\left.\frac{dE}{dx}\right|_{E_0} + \frac{1}{\cos\theta_2}\left.\frac{dE}{dx}\right|_{K_{\rm Bi}E_0}. \tag{7}$$

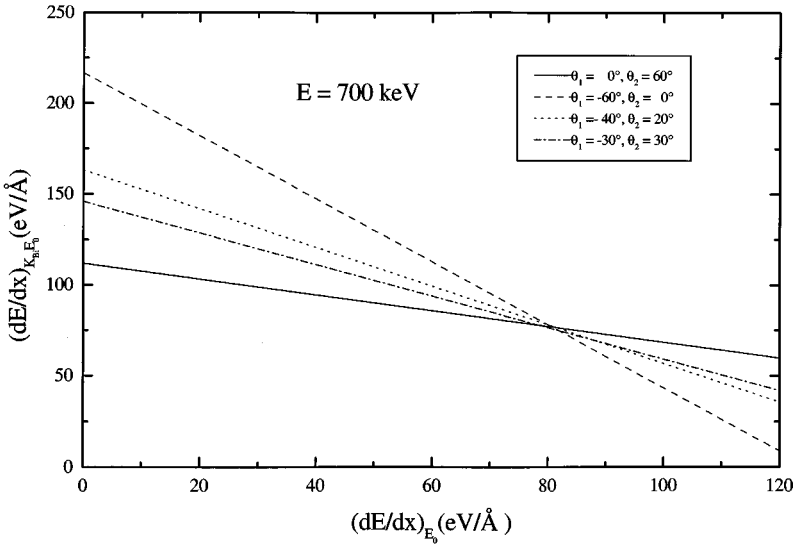

FIG. 3. $(dE/dx)|_{E_0}$ versus $(dE/dx)|_{K_{\mathrm{Bi}}E_0}$ plot for ^{10}B in Si at 700 keV. The straight lines correspond to the specified geometries. The intersection point of two straight lines gives the measured dE/dx values along the inward and outward path.

It can be observed from expressions (6) and (7) that at least two measurements of $E(R_p)$ (performed at different geometries) must be done in order to determine the energy loss dE/dx at the E_0 and $K_{\mathrm{Bi}}E_0$ energies. In the present experiment for each ^{10}B energy we have performed four different measurements, changing the angle between the incident beam direction and the sample's normal. For each energy, the set of measurements was repeated several times and the results were reproducible at a 5% level.

2. Data analysis

As mentioned before in the present data analysis we have used the surface energy approximation.[20] This procedure is justified because the Bi marker is located at the very near surface region.

Expression (7) can be rewritten in the following way:

$$\left.\frac{dE}{dx}\right|_{K_{\mathrm{Bi}}E_0} = m\left.\frac{dE}{dx}\right|_{E_0} + n, \tag{8}$$

with $m \equiv -K_{\mathrm{Bi}}(\cos\theta_2/\cos\theta_1)$ and $n \equiv [S(B)]_{\mathrm{Bi}}^{\mathrm{Si}}$.

By changing θ_1 and/or θ_2 a family of straight lines in the $(dE/dx)|_{E_0}$ versus $(dE/dx)|_{K_{\mathrm{Bi}}E_0}$ plane can be obtained. The intersection of two straight lines gives—for each ^{10}B energy—the corresponding $(dE/dx)|_{E_0}$ and $(dE/dx)|_{K_{\mathrm{Bi}}E_0}$ values.

In order to minimize the errors we have modeled the experiment. This was done by choosing θ_1 (and consequently θ_2) to obtain the maximum possible angle between the straight lines. We have performed for each ^{10}B energy, four experiments under different geometrical conditions. A typical $(dE/dx)|_{E_0}$ versus $(dE/dx)|_{K_{\mathrm{Bi}}E_0}$ plot for ^{10}B at 700 keV is displayed in Fig. 3.

It should be noted that, for each energy there are at most six sets of different $(dE/dx)|_{E_0}$ and $(dE/dx)|_{K_{\mathrm{Bi}}E_0}$ values which arise from the indefiniteness of the intersection point. Then, we have taken the corresponding mean values and those are the ones further quoted. The errors were calculated taking into account (a) the statistical dispersion and (b) the reported uncertainties in the He stopping power.[21]

III. RESULTS AND DISCUSSIONS

A. Channeling stopping powers

According to the procedure outlined in Sec. II A 2 we have determined the energy loss of channeled ^{10}B ions along the ⟨100⟩ Si direction. Figure 4 shows our results for the channeling stopping power as a function of the ion energy. The channeling stopping power increases from 42.4 eV/Å at about 50 keV/amu to 79.7 eV/Å at around 500 keV/amu. Then, it steadily decreases down to 62 eV/Å at 900 keV/amu. The broad maximum in the channeling stopping power around 500 keV/amu probably arises from the maximum in the contribution of the L shell to the electronic stopping power as indicated by plane wave Born approximation (PWBA) calculations.[22]

In the same figure, and for comparison we have plotted the previous results obtained by Eisen,[5] La Ferla *et al.*,[6] and Bogen *et al.*[7] The data point of Eisen[5] at 12.8 keV/amu and the lower energy points of La Ferla *et al.*[6] are out of the presently studied energy range. On the other hand, the high-

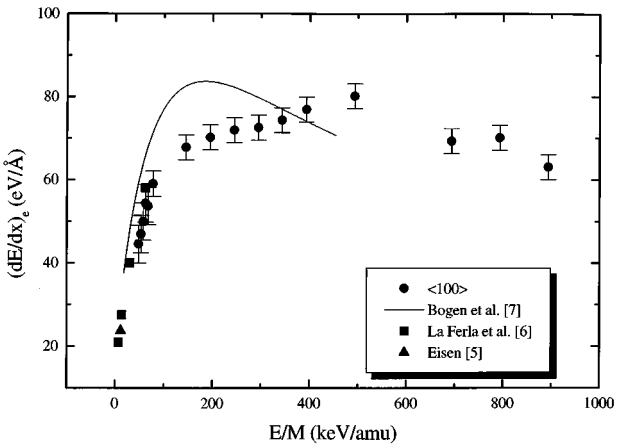

FIG. 4. Channeling stopping powers of ^{10}B in Si ⟨100⟩ as a function of the energy. Full circles correspond to the present results. Full line are the data of Bogen *et al.* (Ref. 7). Squares correspond to the data of La Ferla *et al.* (Ref. 6). Triangle is the data point of Eisen (Ref. 5).

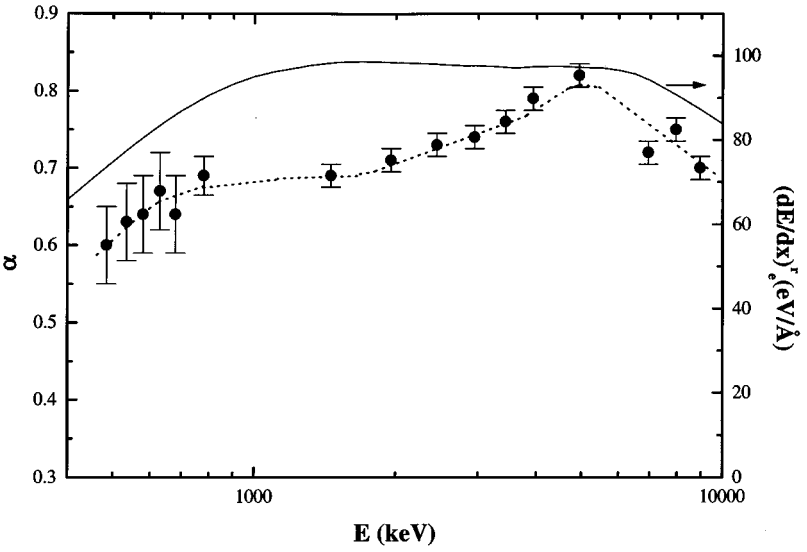

FIG. 5. The full line represents the random stopping power of ^{10}B in Si. The full circles represent the α ratio between the channeling and the corresponding random stopping powers (the dashed line is only to guide the eye).

est energy point of Ref. 6 is in good agreement with the present data. It is pointed out that the data of Bogen *et al.*[7] are systematically higher than the present and previously published data. The reason for this behavior is unknown. It should be noted however, that the indirect procedure, used in Ref. 7 (based on range measurements) could be responsible for the observed discrepancies.

In Fig. 5 we show the α ratio between the channeling and random stopping powers (full circles) as well as the ^{10}B random stopping power as extracted from Ref. 1 (solid line). It can be observed that the α ratio is weakly dependent on the ion energy. Its value ranges from 0.6 at 500 keV up to 0.82 at $E=5000$ keV and decreases to 0.72 at 9000 keV.

We have calculated, on the basis of the free electron model,[17] the contribution to the electronic stopping power of the valence electrons scattered by the effective potential of the moving ion. In principle, this procedure is only valid for a degenerate electron gas. However, for ^{10}B ions of hundreds of keV energy, the projectile maximum energy transfer to the target electrons is high enough (in comparison to the gap width) and, therefore, the effect of the band gap can be neglected. The atomic potential responsible for the scattering of the target electrons was calculated according to the Hartree-Fock-Slater method.[23] Here the long Coulomb range part of the potential has been exponentially screened by the valence target electrons, according to the Debye screening.[24] The calculations of the transport cross section and the electronic energy loss through the phase shifts method[17] were carried out for a 2+ charge state, which according to Betz[25] should be the equilibrium charge state for the present energy range. In addition, we have repeated the calculations for the B neutral charge state which is the equilibrium one for $v\rightarrow 0$.

The results of the calculations are presented in Fig. 6 as a function of the ion velocity ratio, v/v_0 (being v_0 the Bohr velocity). In addition the present (up to 800 keV) and previously published results[5,6] are shown. An inspection of this figure shows several interesting features. First, up to $v/v_0\approx 0.8$ the calculations reproduce quite well the experimental data. Second, for increasing velocities ($v/v_0\geqslant 0.8$) two different behaviors appear: the calculated values which show a broad maximum around $v/v_0=1.6$, whereas the experimental data increase with increasing velocity. Third, for all the studied energy range, there is no significant difference between the calculations performed with charge 2+ or a neutral one. Fourth, the experimental points can be fitted with a power law expression—dash-dotted line—which gives the following result: $dE/dx=(35\pm 1)(v/v_0)^{0.90\pm 0.06}$ eV/Å. The above mentioned features clearly show that the basic energy-loss mechanism for low velocities ($v/v_0\leqslant 0.8$) is due to the scattering of the target valence electrons by the effective potential of the incoming ion. For higher velocities ($v/v_0>0.8$), the difference between the experimental and theoretical results is attributed to other energy-loss contributions such as excitation and/or ionization of inner-shell electrons as well as capture and/or loss of electrons by the ^{10}B ions. In addition it should be observed that for $v/v_0=1.5$, the scattering of the valence electrons by the projectile is responsible for 80 % of the total energy loss. Finally, it should be pointed out

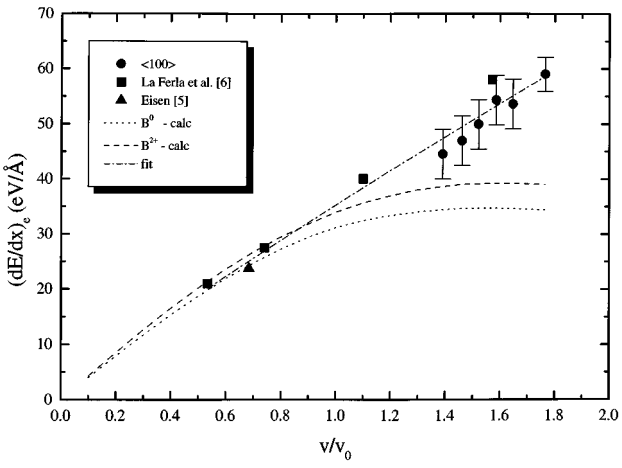

FIG. 6. Calculated electronic stopping powers (for a 2+ and neutral charge state) as a function of the ion velocity ratio, v/v_0 (being v_0 the Bohr velocity). In addition are shown the present (up to 800 keV) and previously published experimental results (Refs. 5 and 6) for the channeling energy loss. All the experimental points were fitted with a power law expression—dash-dotted line—$dE/dx=(35\pm 1)(v/v_0)^{0.90\pm 0.06}$ eV/Å.

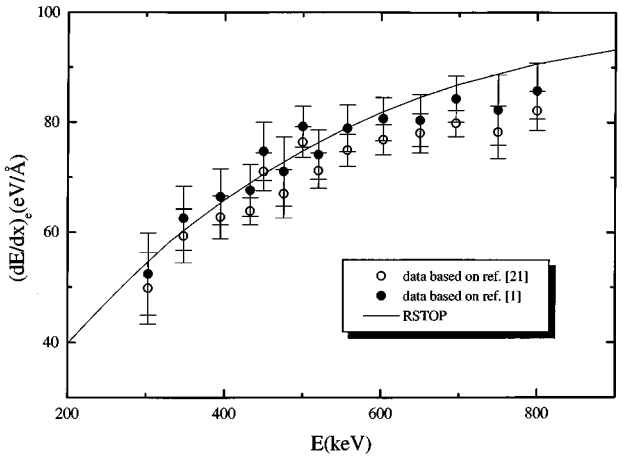

FIG. 7. Random electronic stopping power of ^{10}B in Si. Full line corresponds to the values extracted from Ref. 1. Open circles are present experimental results obtained using the He stopping powers of Ref. 21—see text. Full circles are present experimental results obtained using the He stopping powers of Ref. 1—see text.

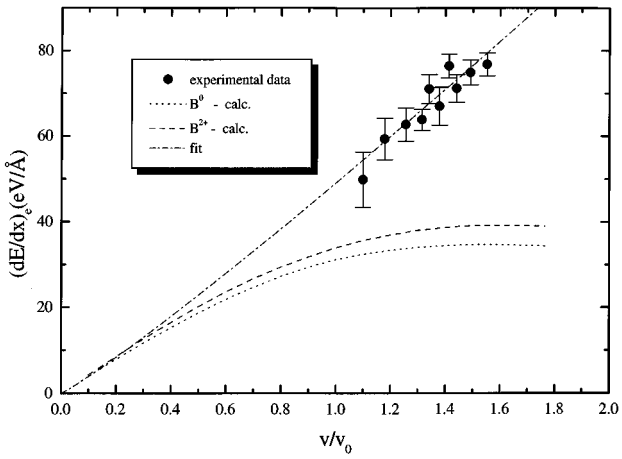

FIG. 8. Low energy random stopping power as a function of the ion velocity together with the calculated electronic stopping powers. The straight dash-dotted line is a fit through the experimental points—see text—which yields: $dE/dx=(49\pm3)(v/v_0)^{1.1\pm0.2}$ eV/Å.

that the whole set of data follows an almost linear relationship with the ion velocity, as predicted by current theories.[11–16]

B. Random stopping powers

In Fig. 7, the ^{10}B random stopping powers obtained in the present experiment in the 300–800 keV energy range are shown. The open circles represent our experimental data whereas the full circles were obtained by recalculating our data using the He stopping powers from the Ziegler, Biersack, and Littmark (ZBL) procedure.[1] The typical error bars in the first case are of the order of 7% being a little bit higher (9%) for the second one due to the larger reported He energy loss uncertainties. In addition, we show with a full line the ^{10}B random stopping data obtained from the RSTOP subroutine.[1]

An inspection of Fig. 7 shows some interesting features. In first place, the ^{10}B random stopping powers deduced from the ZBL (Ref. 1) He stopping powers are systematically higher (by around 5%) than those deduced from Niemann *et al.*[21] This is a consequence of the fact that the reported He stopping power values by Niemann *et al.*[21] in the present studied energy region are about 7.5% lower than the ones of Ref. 1. In second place, the good agreement between the ^{10}B random stopping data extracted from the RSTOP subroutine (full line) and the present experimental one (deduced with the ZBL He data) should be noted. Only at energies higher than 650 keV are slight but systematic differences of around 5% observed.

This last feature can be also deduced from the ^{10}B range measurements in amorphous silicon. In the work of Behar *et al.*,[26] the ^{10}B projected ranges and range stragglings in a 9.5–2000 keV energy interval were investigated. For energies lower than 500 keV the agreement between the experimental projected ranges and the TRIM predictions was better than 2%. However for energies higher than 700 keV the experimental R_p became larger than the predicted ones, being the difference of the order of 6–10 %. These results were very much consistent with the ones obtained by Oosterhoff.[27] This means that the ^{10}B stopping powers of the RSTOP subroutine are larger than the ones which result from the range measurements. These observations are in full agreement with the present results.

In Fig. 8, we have plotted the calculated values from Fig. 6 and our lower energy (300–650 keV) experimental results as a function of the ion velocity. There are not low enough energy experimental data in order to make a meaningful comparison. However, we can emphasize one major point. In the present case and for the same velocity, the theoretical-experimental difference is much larger than the one observed for the channeling case. In particular, for $v/v_0=1.5$ the experimental random value is twice the calculated one, while in the channeling experiments, it was only around 1.25—see Fig. 6. This means that in the random case, the contribution of the excitation and/or ionization processes of inner-shell electrons is much larger—as expected—than in the channeling one.

Finally, we want to state that a least square fit to the data presented in Fig. 8 yields $dE/dx=(49\pm3)(v/v_0)^{1.1\pm0.2}$ eV/Å. This velocity dependence is also in good agreement with the predictions of current theories.[11–16]

Regarding the ^{10}B channeling stopping-power results, it should be pointed out that we have used as input the ^{10}B random energy loss extracted from the RSTOP subroutine—see Sec. II A 2. This was due to the fact that the present measured random stopping values only correspond to a very narrow (300–800 keV) energy interval as compared to the one needed as input for the channeling results. Considering this fact, it is possible that for higher energies ($E>650$ keV) the channeling stopping powers might be systematically lower by 5% with respect to the present quoted results.

IV. CONCLUSIONS

In the present work we report experimental results of ^{10}B stopping powers along the Si⟨100⟩ axis as well as for random directions by using a backscattering technique. For

the low energy regime, both are nearly proportional to the ^{10}B velocity in agreement with the predictions of the current theories. The high energy channeling data ($E > 1500$ keV) show a maximum around 5000 keV, which likely arises from the maximum in the contribution of the L shell of the Si atoms to the B electronic stopping power.

Calculations based on free electron-gas theory indicate that the most important energy-loss mechanism for the low energy ^{10}B ions comes from the scattering of valence electrons by the incoming projectile. Furthermore, we report ^{10}B in Si experimental random stopping-power data. The present results are in quite good agreement with the ones given by the subroutine RSTOP. Only at energies higher than 650 keV, slight but systematic differences are observed. This feature was also seen in previous ^{10}B in Si range measurements, where experimental-theoretical discrepancies of the order of 6–10 % were observed for energies higher than 700 keV. All these results indicate that for energies higher than 700 keV the ^{10}B random stopping powers compiled in the RSTOP subroutine are 5–10 % larger than the ones deduced from experimental observations.

ACKNOWLEDGMENTS

This work was partially supported by the Brazilian agencies Conselho Nacional de Desenvolvimento Científico e Tecnológico (CNPq) and Fundação de Amparo à Pesquisa do Estado do Rio Grande do Sul (FAPERGS).

[1] J.F. Ziegler, J.P. Biersack, and U. Littmark, in *The Stopping and Ranges of Ions in Matter*, edited by J.F. Ziegler (Pergamon, New York, 1985), Vol. 1, and references therein.

[2] J.H.R. dos Santos, P.L. Grande, H. Boudinov, and M. Behar, in *Ion Implantation Technology—94*, edited by S. Coffa, G. Ferla, F. Priolo, and E. Rimini (Elsevier Science B.V., Amsterdam, 1995), p. 711.

[3] J.H.R. dos Santos, P.L. Grande, H. Boudinov, M. Behar, Chr. Klatt, and S. Kalbitzer, Nucl. Instrum. Methods Phys. Res. B **106**, 51 (1995).

[4] J.H.R. dos Santos, P.L. Grande, M. Behar, H. Boudinov, and G. Schiwietz, Phys. Rev. B **55**, 4332 (1997).

[5] F.H. Eisen, Can. J. Phys. **46**, 561 (1968).

[6] A. La Ferla, G. Galvagno, V. Raineri, R. Setola, E. Rimini, A. Carnera, and A. Gasparotto, Nucl. Instrum. Methods Phys. Res. B **66**, 339 (1992).

[7] S. Bogen, L. Gong, L. Frey, and H. Ryssel, Nucl. Instrum. Methods Phys. Res. B **80/81**, 659 (1993).

[8] V. Raineri, G. Galvagno, E. Rimini, J.P. Biersack, T. Nakagawa, A. La Ferla, and A. Carnera, Radiat. Eff. Defect. Solids **116**, 211 (1991).

[9] H. H. Andersen and J.F. Ziegler, in *The Stopping and Ranges of Ions in Matter*, edited by J.F. Ziegler (Pergamon, New York, 1977), Vol. 3.

[10] F. Janni, At. Data Nucl. Data Tables **27**, 147 (1982).

[11] O.B. Firsov, Zh. Éksp. Teor. Fiz. **36**, 1517 (1959) [Sov. Phys. JETP **36**, 1076 (1959)].

[12] J. Lindhard, Mat. Fys. Medd. Dan. Vidensk. Selsk. **28**, 8 (1954); J. Lindhard and M. Scharff, Phys. Rev. **124**, 128 (1961); J. Lindhard, M. Scharff, and H.E. Schiøtt, Mat. Fys. Medd. Vidensk. Selsk. **33**, 8 (1963).

[13] P.L. Grande and G. Schiwietz, Phys. Lett. A **163**, 439 (1992).

[14] P.M. Echenique, R.M. Nieminen, and R.H. Ritchie, Solid State Commun. **37**, 779 (1981); P.M. Echenique, R.M. Nieminen, J.C. Ashley, and R.H. Ritchie, Phys. Rev. A **33**, 897 (1986).

[15] P. Sigmund, in *Interaction of Charged Particles with Solid and Surfaces*, Vol. 271 of *NATO Advanced Study Institute, Series B: Physics*, edited by A. Grass-Marti, H.M. Urbassek, N.R. Arista, and F. Flores (Plenum, New York, 1991), and related papers.

[16] G. Schiwietz and P.L. Grande, Nucl. Instrum. Methods Phys. Res. B **90**, 10 (1994).

[17] K. Schönhammer, Phys. Rev. B **37**, 7735 (1988); P.M. Echenique and M.E. Uranga, in *Interaction of Charged Particles with Solid and Surfaces* (Ref. 15), and references therein.

[18] K. Izumi, M. Doken, and H. Ariyoshi, Electron. Lett. **14**, 593 (1978).

[19] A. Dygo, W.N. Lennard, and I.V. Mitchell, Nucl. Instrum. Methods Phys. Res. B **84**, 23 (1994).

[20] W.K. Chu, J.W. Mayer, and M.A. Nicolet, *Backscattering Spectrometry* (Academic Press, New York, 1978).

[21] D. Niemann, P. Oberschachtsiek, and S. Kalbitzer, Nucl. Instrum. Methods Phys. Res. B **80/81**, 37 (1993).

[22] P.L. Grande and G. Schiwietz (unpublished). The first-order Born calculations were performed for B^{q+} + Si with scaled hydrogenlike projectile wave functions, and target screening was accounted for.

[23] F. Herman and S. Skilmann, *Atomic Structure Calculations* (Prentice-Hall, Englewood Cliffs, NJ, 1963). The numerical calculations of the e-projectile potential was calculated using the NUM program (Ref. 16).

[24] C. Kittel, *Introduction to Solid State Physics* (Wiley, New York, 1986).

[25] H.-D. Betz, Rev. Mod. Phys. **44**, 465 (1972).

[26] M. Behar, P.F.P. Fichtner, P.L. Grande, and F.C. Zawislak, Mater. Sci. Eng. Rep. **15**, 1 (1995).

[27] S. Oosterhoff, Nucl. Instrum. Methods Phys. Res. B **30**, 1 (1988).